

# MEASUREMENTS OF THE RADIAL ELECTRIC FIELD AT ASDEX UPGRADE

S. de Peña Hempel, H. Meister, A. Kallenbach, A. Peeters and ASDEX Upgrade Team

*MPI für Plasmaphysik, EURATOM Association  
D-85748 Garching, Germany*

## 1. Introduction

In a fusion plasma the radial electric field  $E_r$ , which is associated with a reduction in turbulence through sheared  $E \times B$  flow stabilization and a subsequent improvement in confinement, is related to a mutual interaction between the cross field heat and particle transport ( $\nabla p_i$ ), the cross field angular momentum transport ( $v_\phi$ ) and the poloidal velocity  $v_\theta$ . There are several feedback loops whereby  $E_r$  and its shear can change and affect the confinement properties of plasma. For example, an increased shear in the  $E \times B$  drift can lead to a suppression of fluctuations and hence to a reduction in the radial transport, a subsequent steepening of the pressure gradient and thereby to a modification of the electric field itself. To provide insight into the interplay between the different processes, the radial electric field can be inferred indirectly from spectroscopical measurements using the radial component of the momentum balance equation  $E_r = \frac{1}{Z_i e n_i} \nabla p_i + v_\phi B_\theta - v_\theta B_\phi$ . Since this  $E_r$  evaluation indeed neglects the contribution of the inertial terms to the balance equation, it has to be applied with some care and the approximation made has to be verified for each single case.

To measure the poloidal rotation a new spectroscopic diagnostic has been installed at the ASDEX Upgrade tokamak and a deconvolution procedure has been developed and applied in order to recover the radial spatial resolution that is lost due to the integration of the spectral emissivity along the lines of sight. This paper presents first measurements of helium  $v_\theta$  profiles and  $E_r$  in the centre of ASDEX Upgrade plasmas and their connection to the formation of core transport barriers in enhanced reversed shear (ERS) plasmas.

## 2. Diagnostics

The time evolution and the spatially resolved profiles of the impurity ion density  $n_i$ , ion temperature  $T_i$  and toroidal rotation velocity  $v_\phi$  in the core plasma of the ASDEX Upgrade tokamak are routinely monitored in neutral beam heated discharges using the toroidal charge exchange recombination spectroscopy (CXRS). In addition, in order to determine the last term in the balance equation a measurement of the poloidal velocity is necessary. For this purpose a second, high throughput CXRS-system with viewing chords that look (both down and up) across the path of a heating neutral beam has been designed and installed to measure the helium and carbon poloidal rotation.

The sightline geometry is chosen to minimize the effects that emerge from the energy dependence of the excitation rate coefficient for the observed spectral line and simultaneously to maximize the radial resolution within the experimental constraints due to the restricted diagnostic access. Even so, the CX-cross-section effects can significantly distort the apparent poloidal rotation profile when not properly treated.

## 3. Atomic physics effects on the measured line shape

The measured charge exchange emission spectra are strongly affected by the dependence of the CX-cross-section on the relative energy of the beam neutrals and the observed impurity ions, as well as by the Zeeman splitting and the fine-structure components. The clearest manifestation of these effects is an additional shift in the line position and a modified Doppler width, which depend sensibly on the observation angle, magnetic field, beam energy, plasma rotation and ion

temperature. This leads to apparent velocities and temperatures that can greatly differ from the real values.

Since the plasma geometry in ASDEX Upgrade is not up-down symmetric it is not possible to separate the Doppler shift and broadening from these atomic effects by the subtraction of opposing views as is done in other experiments. Therefore they need special consideration and must be taken into account in the analysis during the inversion procedure.

The Zeeman splitting of the energy levels and the apparent non-thermal line broadening caused by this effect are included using the corrective derating factors  $\eta_{\text{Zeeman}}$  described in [1], additionally scaled for arbitrary transition levels  $n$ , ion charges  $Z$  and magnetic fields  $B_{\text{mag}}$ , and modified to take into account the increasing contribution of the  $\sigma$ -component for non-perpendicular viewing geometries. For convenience of computation the  $\eta_{\text{Zeeman}}$  have been parametrized independently of the measured temperature.

Due to collisional  $l$ -mixing not only a single emission line will occur after charge exchange transfer but the whole set of allowed transitions between the  $l$ -levels of the upper and the lower shell will be observed simultaneously. The superposition of each of these fine structure components to form the measured sum profile is calculated by using their correct central wavelengths and relative intensities as available from computations of the ADAS (Atomic Data and Analysis Structure [2]) code for a given parameter set ( $E_{\text{Beam}}$ ,  $n_e$ ,  $n_i$ ,  $T_e$ ,  $T_i$ ,  $Z_{\text{eff}}$  and  $B_{\text{mag}}$ ). However, since the single wavelengths differ only very slightly the resulting line shape can be essentially approximated by a single Gaussian, whose width and peak position define an apparent temperature and an apparent velocity. These are obtained by applying a least squares fit to the ADAS result for each parameter set and are summarized in a structured output for further calculations.

The cross section effects are solved analytically using the algebraic expressions presented in [3], with readily available input parameters, such as observation angle, beam energy, plasma rotation and ion temperature.

#### 4. Inversion Concept

The line-integrated  $v_\theta$ -measurements described in the previous section sample an extended radial range due to the relative height of the neutral beams compared to the poloidal curvature radius of the flux surfaces. In order to recover this lost radial spatial resolution a flexible deconvolution technique has been developed.

The standard matrix inversion method of the Abel integral equation, which assumes rotational symmetry and isotropic emission, is adapted to handle the variation of the emission arising from the neutral beam (necessary to measure the fully stripped impurity ions in the plasma core) and an anisotropic spectral emissivity by introducing a weighted length matrix  $\mathbf{W}_{ijk}$  which relates an emissivity vector,  $E_j$ , to the measured brightness vector,  $B_i$ , by the matrix multiplication  $B_i = \sum_{jk} \mathbf{W}_{ijk} E_j$ . According to [4] the index  $i$  refers to a sightline, the index  $j$  designates the zones of equal poloidal flux and the index  $k$  additionally partitions the plasma into zones of different neutral beam density. The emissivity profile is readily calculated by inverting the length matrix. Expanding the basic idea of the inversion concept developed by R.E.Bell [4] by making a proper redefinition of  $\mathbf{W}_{ijk}$ ,  $E_j$  and  $B_i$  various quantities as the impurity density vector  $n_j^{\text{imp}}$ , the toroidal rotation  $v_j^\phi$ , the poloidal flow velocity  $v_j^\theta$  and the ion temperature  $T_j^{\text{imp}}$  can successively be determined from the charge exchange measurements taking into account specific geometry factors and the contribution of several neutral beams.

First, a length matrix,  $\mathbf{W}_{ijk} = \mathbf{L}_{ijk} n_{ijk}^{\text{beam}} \langle \sigma^{\text{CX}} v \rangle_{ijk}^{\text{eff}}$  can be defined, which contains the vertical and the radial variations of the neutral beam density  $n_{ijk}^{\text{beam}}$  determined from an independent beam attenuation calculation, the effective charge exchange rate  $\langle \sigma^{\text{CX}} v \rangle_{ijk}^{\text{eff}}$  and the length

of the viewing chord in a given zone  $L_{ijk}$ . By inverting this matrix the impurity density vector can be obtained from the measured brightness vector,  $B_i^{CX}$ .

Next the flow velocity is deconvolved by solving  $(B_i^{CX} u_i^{CX}) = \sum_{jk} \mathbf{E}_{ijk}^{CX} (v_j \Theta_{ij}^z + \Delta \lambda_{ijk}^{CX})$ , where  $u_i$  is the apparent rotation velocity,  $\mathbf{E}_{ijk}^{CX} = \mathbf{W}_{ijk} n_j^{imp}$  is the integrated local emissivity for the particular viewing geometry being considered and  $\Theta_{ij}^z$  contains directional information of the velocity vector. A calculation of a matrix of cross section and fine structure shifts  $\Delta \lambda_{ijk}^{CX}$  is also assumed, which requires measurements of  $T_j^{imp}$  and the velocity vector itself. However, as next to no effect can be found from the cross section effect on the deduced ion temperatures, a first approximation of  $T_j^{imp}$  is obtained by mapping the measured values onto a mean poloidal flux label defined as  $\langle \rho \rangle_i = \sum_{jk} \rho_{ijk} \mathbf{E}_{ijk}$ . Further, since the magnitude of the expected poloidal velocity is typically more than an order of magnitude smaller than the toroidal velocity, its contribution to the correcture term for  $v_\phi$  has not to be considered in practise. So, assuming no flow in radial direction, the velocity vector can accurately be determined without the need of any iteration by following a two step procedure: first the toroidal rotation is inverted neglecting the effect of  $v_\theta$  and then the poloidal velocity is deconvolved from the measurements of the vertical CX-system after recalculating  $\Delta \lambda_{ijk}^{CX}$  with the inferred  $v_\phi$ .

Finally, the impurity ion temperature profile can be obtained from the evaluation of  $B_i^{CX} \left[ \frac{kT_i^{CX}}{mc^2} + \frac{\lambda_0^2}{c^2} u_i^{CX2} \right] = \sum_{jk} \mathbf{E}_{ijk}^{CX} \left( \frac{kT_j^{imp}}{mc^2} + \frac{\lambda_0^2}{c^2} [v_j \Theta_{ij}^z + \Delta \lambda_{ijk}^{CX}]^2 \right)$ .

As the presented matrix inversion procedure is very sensitive to the gradient of the brightness, to handle real data with errors it is combined with a curvature and error minimization procedure based on the regularization method of Tikhonov [5].

## 5. Results

Here the phenomenology of core barrier dynamic in an Enhanced Reverse Shear (ERS) plasma at ASDEX Upgrade is examined by means of first measurements supplied by the new spectroscopic diagnostic and the implemented deconvolution procedure.

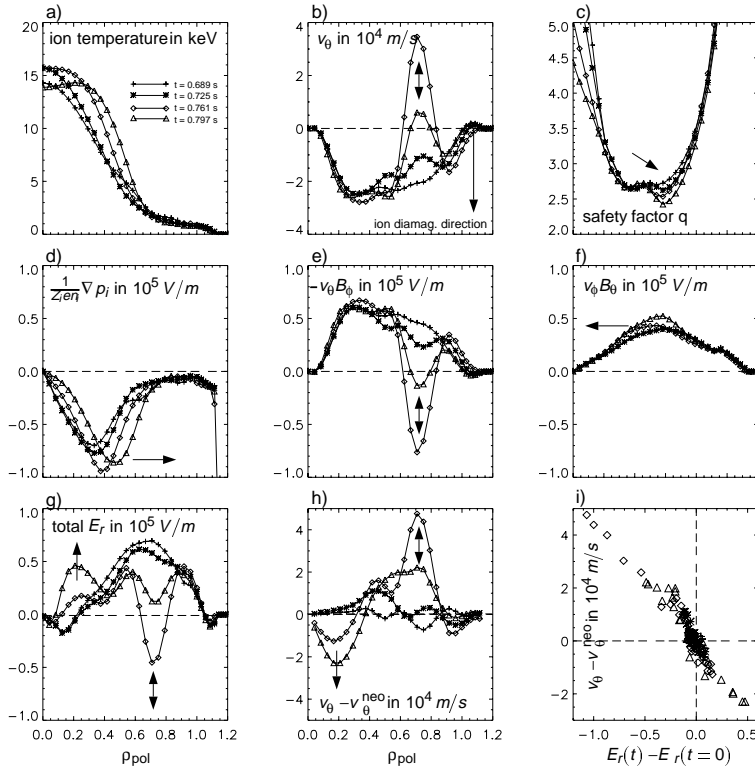


**Figure 1.** The eight first pictures show the temporal evolution of the ion temperature profile a), the poloidal rotation velocity b), the safety factor c), the different contributions d), e), f) to the total radial electric field  $E_r$  g) and deviation of the measured  $v_\theta$  from neoclassical predictions h) during the ERS transition of discharge #10701. Finally, in picture i)  $v_\theta - v_\theta^{neo}$  is plotted versus the measured change in  $E_r$  for all the times and radii.

The presented discharge (#10701) is seen to undergo an enhancement in its confinement characteristics shortly after the start of the neutral beam heating phase, as indicated by the steepening of the helium temperature profile in Fig. 1 a). The onset of the core transport barrier is accompanied by a localized spontaneous excursion of the poloidal velocity from the helium ions originally rotating in the ion diamagnetic drift (negative) direction (Fig. 1 b)). As the extent of this velocity shear region is small compared to the radial separation of the vertical sightlines, the width of the reversal region and the full magnitude of the positive velocity obtained from the deconvolved data can be strongly disturbed by the resolution of the system. Though, the radially deconvolved  $v_\theta$  profiles indicate that this flow reversal is clearly localized outside the region that ultimately becomes the transport barrier region but very close to the minimum in the safety factor profile,  $q$  (Fig. 1 c)), as derived self-consistently from ASTRA code calculations.

The dynamic of the enhanced core confinement is characterized by a propagation of the transport barrier, as defined by the change in the slope of the ion temperature, and the location of  $q_{\min}$  outward with time. This expansion is maintained during the period of  $v_\theta$  reversal and stops as the poloidal rotation returns to its initial value after the confinement transition.

Since the  $v_\theta$  excursion precedes measurable deviations in other background plasma profiles, its contribution (Fig. 1 e)) dominates the spontaneous decrease of the plasma  $E_r$  (Fig. 1 g)) early in time. As described in [6] this indicates the change in  $E_r$  shear to be a causal element of the confinement bifurcation and points to its threshold character. As the flow reversal subsequently relaxes and the transport barrier moves outward, the diamagnetic contribution to the radial electric field (Fig. 1 d)) cannot compensate the term  $v_\phi B_\theta$  (Fig. 1 f)) in the plasma core any longer, leading to an enhancement of  $E_r$  in this region. Contrary to the fast  $v_\theta$ -activity outside the steep gradient region, the increased central electric field strength is sustained during the entire period of enhanced confinement.

Poloidal flow evaluations from steady state neoclassical considerations [7] that describe the measured profiles quite accurately during the period of lower confinement, however cannot predict the dynamics of the large poloidal velocity and the velocity shear observed. Therefore the behaviour of  $v_\theta$  in the core deviates from these calculations especially at the bifurcation time (Fig. 1 h)). The difference between the measured and neoclassically predicted  $v_\theta$  exhibits a strong temporal and spatial correlation to the measured change in  $E_r$  (Fig. 1 i)). In the region where this change is dominated by the  $v_\theta B_\phi$  contribution this correlation is trivial. Not so, however, in the central plasma region where the enhancement of the measured radial electric field arises from the displacement of the transport barrier and may be related to an increase of the ion heat diffusion  $\chi_i$  towards the plasma centre [8]. A possible interaction mechanism between  $E_r$  and  $\chi_i$  may be induced through the dependence of  $\chi_i$  on the trapped orbit squeezing factor  $S = 1 - \frac{mc^2}{eB_\theta^2} \frac{\partial E_r}{\partial r}$ ,  $\chi_i \propto S^{-3/2}$ . First estimates show that at the time where the ion temperature flattens in the centre, the squeezing factor  $S$  is significantly smaller than 1, leading to an increase in  $\chi_i$ . Detailed calculation will be addressed in future work.

## References

- [1] R.P. Schorn, E. Wolfrum et al.: Nuclear Fusion **32**, 351–359 (1992)
- [2] H.P. Summers: JET Joint Undertaking Report JET-IR(94)-06, 1994
- [3] M. von Hellermann et al.: Plasma Phys. Control. Fusion **37**, 71 (1995)
- [4] R.E. Bell: Rev. Sci. Instrum. **68**(2), 1273–1280 (1997)
- [5] R. Wunderlich et al.: Max-Planck-Institut für Plasmaphysik Report IPP 5/37, 1992
- [6] E.J. Synakowski et al.: “Formation and structure of internal and edge transport barriers”.  
*Accepted for publication in Plasma Phys. Control. Fusion* (1998)
- [7] Y.B. Kim et al.: Phys. Fluids B **3**(8), 2050–2060 (1991)
- [8] G. Pereversev et al.: *This conference*, 1998